


Article

Sequential Redox Precipitation and Solvent Extraction for Comprehensive Metal Recovery from Spent High Manganese Lithium-Ion Battery

Jiawei Zhang ^{1,2} , Fupeng Liu ^{1,2,*}, Chunfa Liao ^{1,2,*}, Tao Zhang ^{1,2}, Feixiong Chen ^{1,2}, Hao Wang ^{1,2} and Yuxin Gao ^{1,2}

¹ Yichun Lithium New Energy Industry Research Institute, Jiangxi University of Science and Technology, Ganzhou 341000, China

² Jiangxi Provincial Key Laboratory of High-Performance Steel and Iron Alloy Materials, Ganzhou 341000, China

* Correspondence: fupengliu@126.com (F.L.); liaochfa@163.com (C.L.)

Abstract

The traditional recycling process of spent lithium-ion battery (LIB) with high Mn content faces the defects of high cost of neutralization and precipitation, poor economics of Mn extraction, and serious Li loss. Therefore, this paper introduces a comprehensive hydrometallurgical method for extracting valuable metals from high-Mn spent LIB. Particularly, directional precipitation of Mn was achieved by utilizing its redox properties, and shot-process extraction and enrichment of Li was realized by using the extractant HBL121. In a sulfuric acid system, control of the oxidant dosage to 0.8% resulted in high leaching efficiencies for Li, Ni, Co, and Mn, with values of 96.58%, 96.13%, 95.22%, and 94.24%, respectively, under optimal conditions which were $C(H_2SO_4)$ of 3.5 mol/L, $V(H_2O_2)$ of 0.8% (v/v), L/S of 10:1, temperature of 60 °C, and time of 60 min. Subsequently, the addition of $KMnO_4$ dosage (K_p/K_t) in a ratio of 1:1 resulted in the precipitation of 98.47% of Mn as MnO_2 , with Ni and Li precipitation efficiencies of 0.2% and 0.1%, respectively. Cascade extraction of Ni and Co was reached by using Cyanex272 extractant from the solution after Mn precipitation. At an organic-to-aqueous phase ratio (O/A) of 1:5, the Co extraction efficiency reached 98.68%, whereas the loss efficiency of Ni was 5.53%, and Li was less than 0.1%. Adjusting the O/A to 1:1 increased the Ni extraction efficiency to 89.99% and Li loss to 8.95%. Finally, the HBL121 extractant was utilized to extract Li from the Li-rich solution, achieving 95.08% extraction efficiency. The Li was stripped with 2 mol/L H_2SO_4 from the load organic phase, realizing a Li concentration of 11.44 g/L. Thus, this process facilitates the comprehensive and efficient recovery of valuable metals such as Li, Ni, Co, and Mn from spent high-Mn LIB.

Keywords: spent lithium-ion batteries; sulfuric acid leaching; selective separation; precipitation; solvent extraction



Academic Editor: Man Seung Lee

Received: 23 July 2025

Revised: 22 August 2025

Accepted: 25 August 2025

Published: 26 August 2025

Citation: Zhang, J.; Liu, F.; Liao, C.; Zhang, T.; Chen, F.; Wang, H.; Gao, Y. Sequential Redox Precipitation and Solvent Extraction for Comprehensive Metal Recovery from Spent High Manganese Lithium-Ion Battery. *Metals* **2025**, *15*, 948. <https://doi.org/10.3390/met15090948>

Copyright: © 2025 by the authors. Licensee MDPI, Basel, Switzerland. This article is an open access article distributed under the terms and conditions of the Creative Commons Attribution (CC BY) license (<https://creativecommons.org/licenses/by/4.0/>).

1. Introduction

Driven by technological advances and policy support, the rapid adoption of electric vehicles has significantly increased demand for high-performance power batteries. Upon reaching end-of-life, approximately 70% of lithium-ion batteries (LIBs) undergo secondary use in energy storage applications, while those below 30% capacity efficiency are directly

recycled, making decommissioned battery processing critical for resource recovery and environmental management [1–4]. Projections indicate China's end-of-life battery volume will reach 0.5–1 million metric tons by 2030, escalating to 1.5–2.5 million tons by 2050, encompassing power batteries, gradient-utilized storage, and smaller civilian LIBs, underscoring an urgent need for an effective recycling strategy [5]. Spent LIBs contain valuable heavy metals (Ni, Co, Mn, Cu) and organics [6]; improper disposal wastes resources and poses environmental and health risks [6,7]. Furthermore, the fluctuating scarcity and prices of these metals have spurred the industry to explore sustainable resource utilization methods. A recycling process to recover these high-value metals could reduce reliance on primary resources and alleviate environmental burdens.

Current battery recycling primarily utilizes pyrometallurgical and hydrometallurgical methods. Pyrometallurgy, exemplified by high-temperature ($>1450\text{ }^{\circ}\text{C}$) reduction smelting-chlorination [8], volatilizes Li and Mn as chlorides while concentrating transition metals (Cu, Ni, Co) into alloy phases; however, this approach suffers from severe equipment corrosion, high exhaust gas treatment costs, extreme energy consumption, and challenges in recovering Li and Mn. In contrast, hydrometallurgical processes like ammonia leaching selectively extract Co, Cu, and Ni but exhibit slow kinetics and cannot recover Li [9]. Consequently, acid leaching is more favored due to its efficient extraction of Li, Co, and other valuable metals at relatively mild temperatures. Recycling typically begins with acid leaching of cathode materials, followed by impurity removal. Inorganic acids (HCl, HNO_3 , H_2SO_4) are prevalent and effective [1,10,11], with H_2SO_4 + oxidant/reductant systems achieving high leaching efficiencies ($>96\%$) for Li, Ni, Co, and Mn [12,13]. While HNO_3 and HCl can release toxic gases (Cl_2 , NO_x), H_2SO_4 remains predominant due to its efficiency and relatively lower environmental impact [14]. This facilitates the transformation of high-valent metal oxides or metal monomers [15] into metals. Gu et al. [16] employed an innovative leaching system using citric acid and orange peel, achieving over 97% leaching efficiencies for Li, Ni, Co, and Mn. Organic acids offer an eco-friendly alternative but face industrial challenges due to lower acidity and cost.

Following metal recovery, separation techniques such as precipitation, extraction, ion exchange, and electrodeposition are necessary. Extraction and precipitation are the most prevalent, each with specific advantages. Extraction offers high selectivity and recovery efficiency but at a higher cost, while precipitation is simpler and more environmentally benign but less selective and efficient. Common extractants include P507 and Cyanex272 for Ni and Co, with Cyanex272 [17] being more effective. P204 is typically used for Mn, while TBP + FeCl_3 and HBL121 are used for Li. Chunyan [18] utilized dimethylglyoxime (DMG) for Ni precipitation, P204 for Mn extraction, Cyanex272 for Co recovery, and Na_2CO_3 for Li precipitation, achieving recovery efficiencies of 96.84% for Ni, 81.46% for Co, 92.65% for Mn, and 91.39% for Li. Zhang et al. [19] reported a primary Li extraction efficiency of 99% using HBL121, with a post-stripping concentration of 15.56 g/L. Jiang et al. [20] employed ammonium oxalate for co-precipitation, ammonium bicarbonate for Mn, and a sodium carbonate-sodium hydroxide co-precipitation method for Ni and sodium carbonate for Li, achieving efficiencies of 99.17% for Co, 97.88% for Mn, 93.47% for Ni, and 85.21% for Li.

Currently, the recycling of spent LIBs faces multiple challenges, including complex processes, incomplete material recovery, low purity of recovered metals, and [21] managing resultant waste. Despite extensive research on recovering Li, Ni, and Co [22–25], few studies have focused on Mn [26], often regarded as an impurity that complicates the recycling process of spent LIBs. The presence of Mn can interfere with the extraction and purity of Ni and Co [25]. Nonetheless, as a significant metal resource, Mn plays a pivotal role across industrial sectors, particularly as a deoxidizer and desulfurizer in steel production and as an essential component in traditional zinc-manganese batteries. Furthermore, the

recovery of Mn from spent LIBs could contribute significantly to resource sustainability and environmental protection. Lithium, as a strategic metal, holds significant importance on a global scale. First, lithium plays a pivotal role in the development of lithium-ion batteries for electric vehicles, serving as a core component that offers impressive energy density and a long cycle lifespan, making it a key driver for sustainable development. Secondly, global lithium resources are highly concentrated, primarily sourced through mining and electrolytic methods, which exacerbates resource scarcity and environmental pollution issues, thereby necessitating the urgent need for sustainable production and recycling of lithium. The lithium extraction methods are generally categorized into pre-processing recovery [27–30] and post-processing recovery [31,32]. Pre-treatment lithium recovery prioritizes lithium extraction, which may enhance resource utilization efficiency, but it could also result in increased waste generation and harmful byproducts, thereby imposing additional environmental burdens. On the other hand, post-treatment lithium recovery processes exhibit lower environmental pollution and pressure during the recycling process, with the added advantage of concurrent recovery of valuable metals. However, challenges such as high lithium recovery losses and difficulties in lithium concentration remain to be addressed in this approach. Therefore, developing a technology that efficiently recovers Li, Ni, Co, and Mn from high-Mn LIBs could offer substantial socioeconomic and ecological benefits.

Therefore, developing efficient technology for recovering Li, Ni, Co, and Mn from high-Mn spent LIBs offers substantial socioeconomic and ecological benefits. This study proposes a full hydrometallurgical process for high-Mn spent LIBs: (i) metals are collectively leached via a $\text{H}_2\text{O}_2\text{-H}_2\text{SO}_4$ system, (ii) Mn is removed through oxidative precipitation to prevent interference with subsequent Ni/Co extraction and to reduce costs, and (iii) Ni, Co, and Li are sequentially extracted and separated using targeted extractants, followed by lithium enrichment via stripping. This methodology optimizes critical metal recovery while demonstrating significant economic-environmental synergies.

2. Materials and Methods

2.1. Material and Analysis

The raw materials utilized in the experiments were derived from mixed powders of the positive and negative electrodes of spent high-Mn lithium-ion batteries. These materials were sourced from domestic spent lithium battery recycling manufacturers. The chemical composition of the spent LIBs cathode powder is detailed in Table 1. As shown in the table, the Mn content of 18.10% is the highest in the cathode powder, and subsequent separation and recovery of Mn must consider interference with the separation of other elements. Other valuable elements, such as Ni, Co, and Li, also have high content levels, resulting in high overall recovery value.

Table 1. Chemical components of spent high-Mn lithium-ion battery (wt %).

Element	Li	Ni	Co	Mn	Al	Fe	Cu
Content	3.54	10.70	4.41	18.10	2.07	0.88	0.92

X-ray diffraction (XRD) phase analysis was conducted on the spent LIBs cathode powder through step scanning, as illustrated in Figure 1. The analysis revealed that the primary phases within the material are C, LiCoO_2 , and $\text{LiNi}_{0.18}\text{Mn}_{1.82}\text{O}_4$. Owing to their low concentrations, Al, Fe, and Cu did not exhibit distinct peaks in the XRD spectra. The raw material consists of irregularly shaped, unevenly sized fine particles, as shown in Figure 2. Elemental surface scanning analysis (as shown in Figure 3) indicates that the distribution regions of manganese Mn, Ni, Co, and O overlap, forming a composite phase without distinct distribution bound-

aries. In contrast, Al and C exist as independent phases with recognizable phase boundaries, a distribution consistent with the results of XRD analysis.

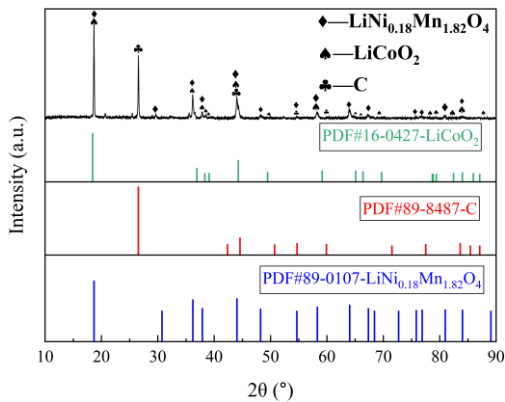


Figure 1. XRD diffractogram pattern of spent high-Mn lithium-ion battery.

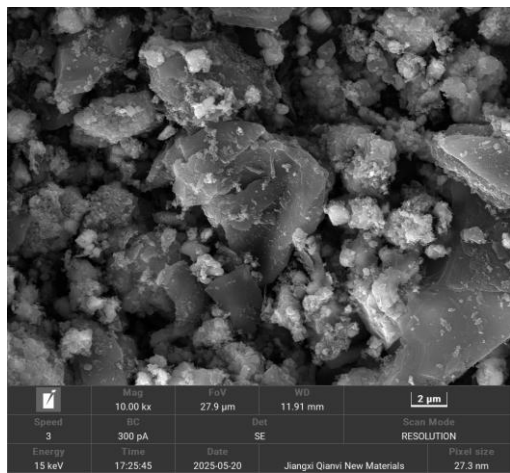


Figure 2. Scanning electron microscope micrographs of spent high-Mn lithium-ion battery.

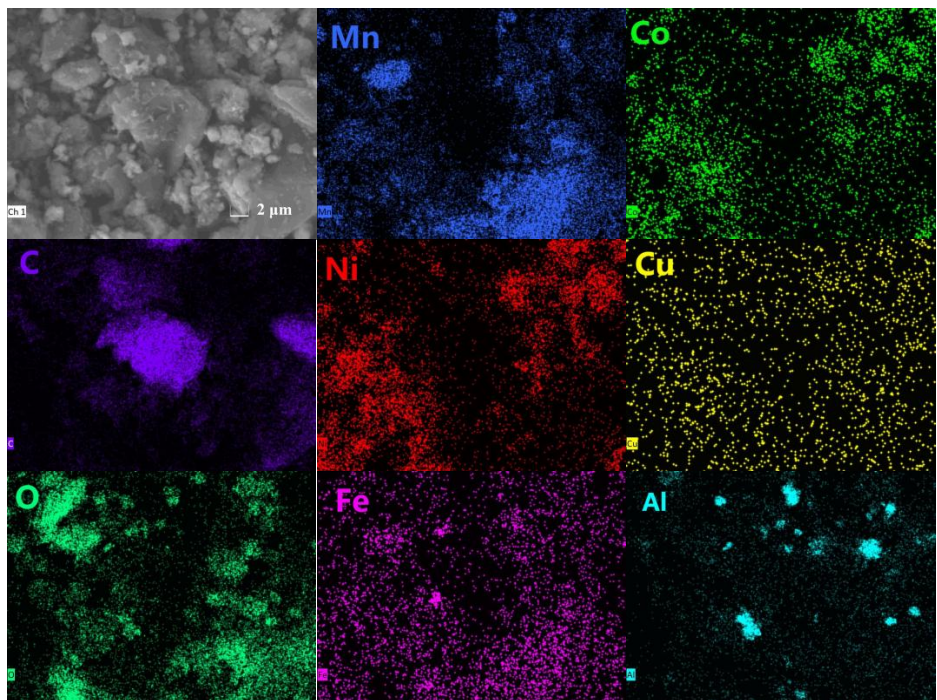


Figure 3. Distribution maps of the main components present in spent high-Mn lithium-ion battery. Ruler.

2.2. Experiment Procedures

The leaching solution, enriched with valuable metals such as Li, Ni, Co, and Mn, was prepared through oxidative leaching using sulfuric acid. This was followed by separating Mn from other metals, such as Li, Co, and Ni, using oxidative precipitation with potassium permanganate. The subsequent step-by-step separation of Ni, Co, and Li involved pH adjustments and the application of extraction techniques. This study also examined the influence of various factors on the leaching efficiency of the metals, including the concentration of sulfuric acid, the concentration of hydrogen peroxide, the liquid-solid ratio of the acid leaching solution, leaching time, and leaching temperature. Additionally, the impact of pH levels and the actual amount of potassium permanganate added were investigated concerning the precipitation efficiency of Mn and the associated loss efficiencies of Li, Ni, and Co.

Following the precipitation process, different extractants, such as P204, P507, and Cyanex272, were utilized to assess their extraction effects. This comparison was crucial to selecting the most suitable extractant for the efficient separation and recovery of Ni, Co, and Li from the solution post-Mn precipitation. The final stage involved using HBL121 to enrich and recover Li through extraction and stripping processes. The complete procedural flow of these steps is illustrated schematically in Figure 4. The solutions before and after each process treatment are named using LAN (n: 1–8).

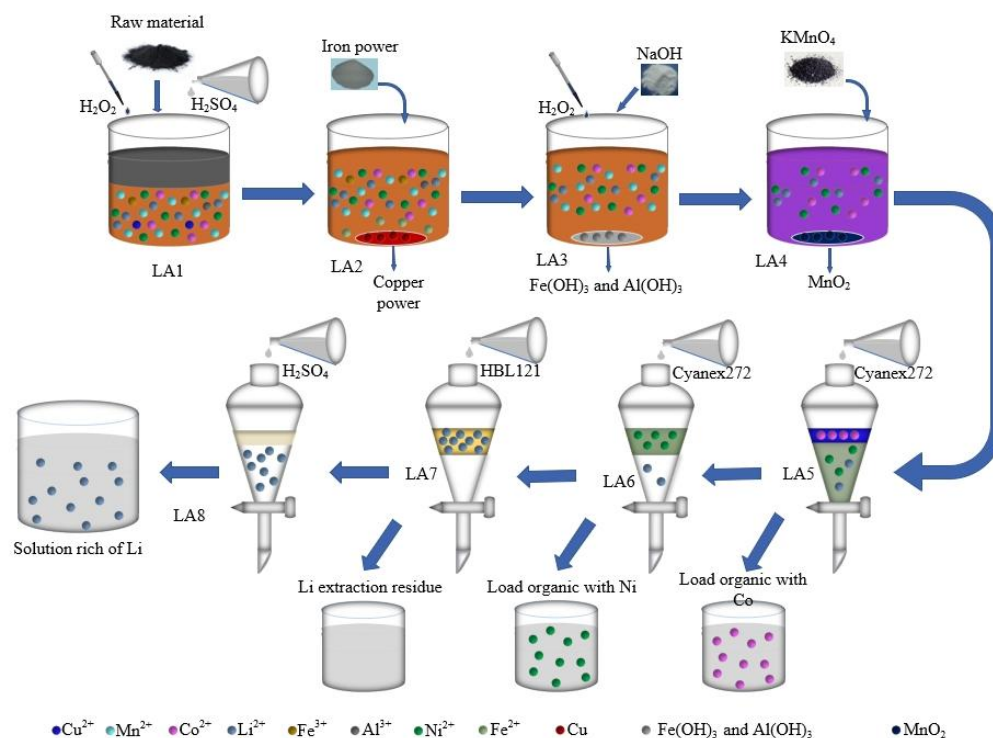


Figure 4. Schematic illustration of the recovery process from high-Mn lithium-ion battery.

2.2.1. Sulfuric Acid-Hydrogen Peroxide Leaching

The precisely weighed raw material was uniformly mixed with sulfuric acid in a beaker, maintaining a specific liquid-to-solid (L/S, mL/g) ratio. Subsequently, a designated concentration of hydrogen peroxide solution was added to the mixture. The primary parameters investigated to optimize the separation of valuable metals included the concentration of sulfuric acid, leaching time, leaching temperature, L/S ratio, and oxidant concentration. Upon completion of the reaction, solid-liquid separation was performed using a vacuum pump (model SHB-III G, Zhengzhou Great Wall Science, Industry and Trade Co., Ltd., Zhengzhou, China). Both the residue and the filtrate were then characterized and analyzed.

The leaching procedure involved heating the mixture in 100 mL flat-bottom flasks equipped with magnetic stirring at 300 rpm. Temperature control was achieved using a water bath (DF-101S, Gongyi Yuhua Instrument Co., Gongyi, China). Unless otherwise specified, the same water bath temperature and stirring conditions were maintained for all subsequent leaching processes. The leaching efficiencies (L (%)) of Li, Ni, Co, and Mn from the leachate were calculated using the specified equation.

$$L(\%) = \left(\frac{Vc}{mW} \right) \times 100 \quad (1)$$

where L (%) is the leaching efficiency; c (g/L) is the concentration of each metal in the leaching solution, V (L) is the volume of the leaching solution, m (g) is the mass of the roasting stock, and W (%) is the concentration of each metal in the roasting stock.

2.2.2. Selective Separation of Mn

To selectively separate Mn, solid KMnO_4 was added to the leachate in a 100 mL glass beaker equipped with a magnetic stirrer, using a specified ratio. The mixture was then heated to 30 °C for 30 min. The precipitation of Ni, Co, Mn, and Al was investigated under various conditions by altering the amounts of KMnO_4 and adjusting the pH values. After these adjustments, the concentration of each metal ion remaining in the leachate was measured using inductively coupled plasma (ICP) spectroscopy. Based on these measurements, the precipitation efficiencies of the metals were calculated to evaluate the effectiveness of the process under different experimental conditions.

The precipitation efficiency of Mn and the loss efficiencies of Li, Ni, and Co were calculated as follows:

$$P(\%) = \left(1 - \frac{c_1 V_1}{c_2 V_2} \right) \times 100 \quad (2)$$

where P (%) is the precipitation efficiency or loss efficiency, c_1 (g/L) is the concentration of elemental Mn in the filtrate after precipitation and filtration, c_2 (g/L) is the concentration of elemental Mn in the solution before precipitation, V_1 (L) is the volume of the precipitated filtrate, and V_2 (L) is the volume of the leachate.

2.2.3. Selective Separation of Ni, Co, and Li

Preliminary saponification: Acidic extractants (such as P204, P507) release H^+ when they come into direct contact with the feed solution, causing a sudden drop in the pH of the system. At this point, some metal ions hydrolyze and precipitate, resulting in losses. Therefore, saponification pretreatment is required before extraction. The prepared extractant is mixed with 10 mol/L NaOH and shaken for 2 min. After standing for 15–30 min, the aqueous phase is separated, and the extractant is washed twice with deionized water to remove residual Na^+ , preventing contamination in subsequent extractions. The saponification rate (%) is calculated as the percentage ratio of the actual NaOH consumption (mol) to the theoretical NaOH requirement (mol). Generally, saponification is performed to achieve a rate of 40–70%. In this study, the saponification efficiencies for P204, P507, and Cyanex272 were 60%, 60%, and 50%, respectively.

Extraction of Ni, Co, and Li: Solvent extraction experiments were conducted by mechanically agitating the organic and aqueous phases in separate funnels. The shaking speed and temperature were regulated using a thermostatic water bath shaker (SHZ-88 Model number, Shanghai Lichen Instrument Technology Co., Ltd., Shanghai, China). For the separation of Ni and Co, the organic and aqueous phases were combined in a 60 mL separatory funnel at a predetermined volume ratio and agitated at 30 °C for 20 min. The separation performance of Li, Ni, and Co was assessed using different extractants (P204,

P507, and Cyanex272) under varying phase ratios and pH conditions. In the Li enrichment experiments, the solution derived from the Ni and Co separation was blended with the organic phase at a specified ratio and agitated in a water bath at 30 °C for 20 min. Subsequently, phase segregation was allowed after a settling period of several minutes. The concentrations of metal elements in the aqueous phase were analyzed, and the concentrations of metal ions in the organic phase were calculated based on the mass balance of the metal ions in the aqueous phase.

The formula for extraction ($E\%$) was as follows:

$$E(\%) = 100 \times \frac{c_3 - c_4}{c_3} \quad (3)$$

where E (%) is the extraction efficiency, c_3 (g/L) is the concentration of the metal in the solution before extraction, and c_4 (g/L) is the concentration of the metal in the solution after extraction.

2.3. Analysis and Characterization

The elemental contents of Li, Ni, Co, Mn, Al, Fe, and Cu in both the spent high-Mn LIBs melting sample and the leaching solution, as well as the elemental content in the aqueous phase before and after extraction, were analyzed using a thermo ICAP-AES 7400 ICP emission spectrometer (Model ICAP-AES 7400, Thermo Fisher Company HORIMA, Waltham, MA, USA). Phase compositions of the raw material, leach slag, and Mn precipitation slag were determined using an X-ray diffractometer (Cu target, $K\alpha_1 = 1.5406 \text{ \AA}$, scanning speed $10^\circ/\text{min}$, scanning angle $10\text{--}90^\circ$) of X'pert Powder type, Spectrum, Panaco, XRD-6000, Shimadzu Company, City Kyoto, Japan. The micromorphology and regional elements of the raw material and Mn precipitation slag were characterized with a field-emission scanning electron microscope (MIRA 3 LMH, TESCAN ORSAY HOLDING Company, City Brno, Czech Republic).

3. Results and Discussion

3.1. Sulfuric Acid-Hydrogen Peroxide Leaching

Experiments were conducted under one-factor-at-a-time conditions to assess the impact of various factors on the leaching efficiency of metals such as Li, Ni, Co, and Mn, among others. In these experiments, sulfuric acid concentration (0.5–4.5 mol/L), hydrogen peroxide concentration (0.2–1.1%, v/v), L/S ratio (4:1–12:1), leaching temperature (20–80 °C), and leaching time (15–75 min) were varied. The results of these studies are presented in Figure 5.

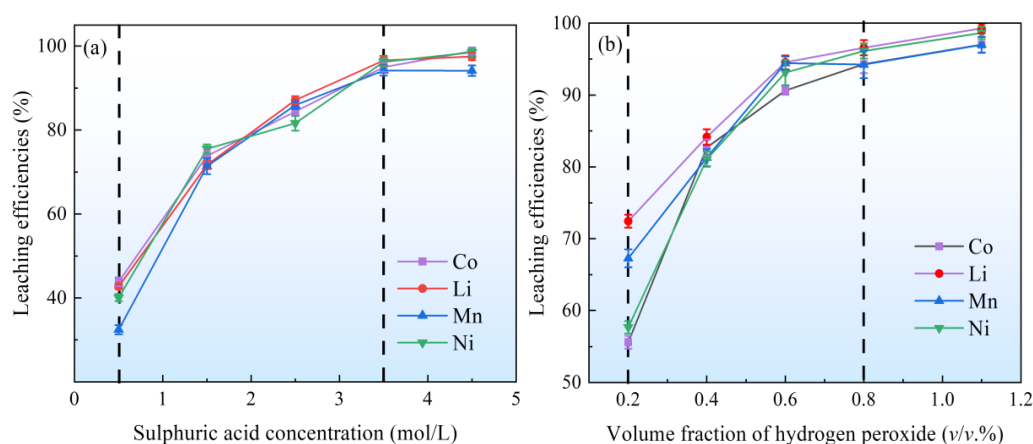


Figure 5. Cont.

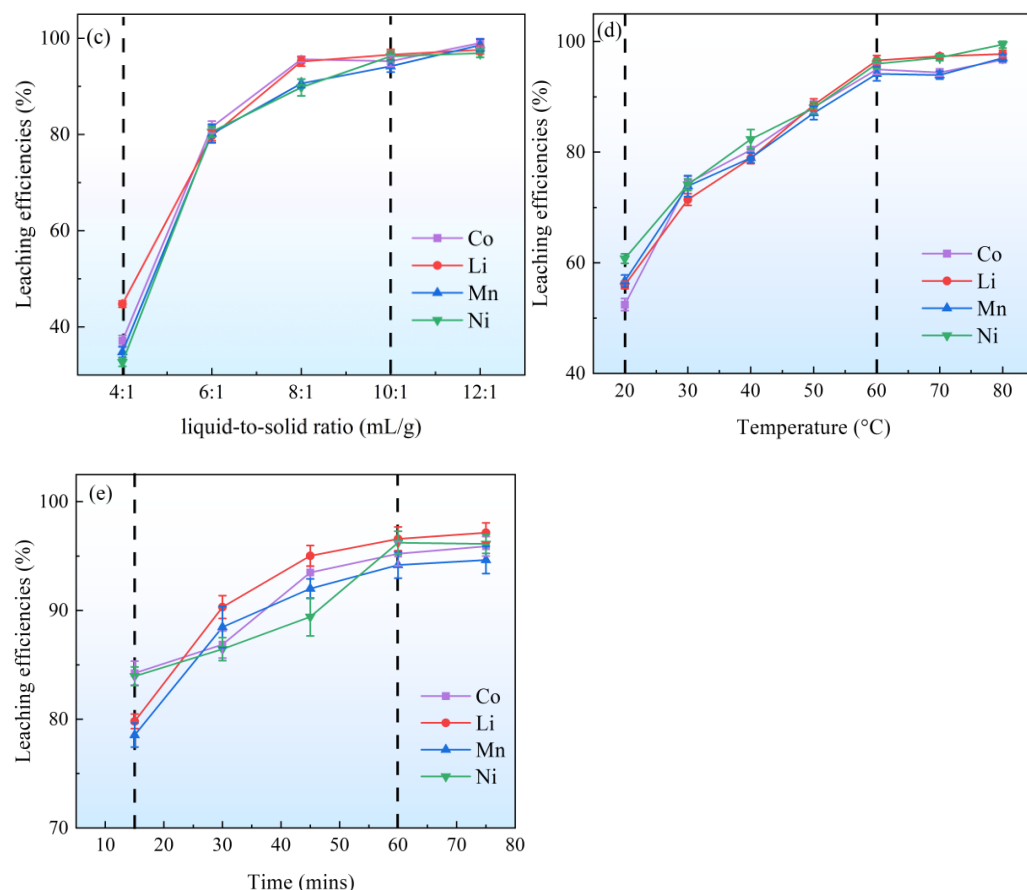


Figure 5. Effect of (a) sulfuric acid concentration ($V(\text{H}_2\text{O}_2) = 0.8\%$ (v/v), $L/S = 10:1$, $T = 60\text{ }^\circ\text{C}$, $t = 60\text{ min}$); (b) hydrogen peroxide concentration ($C(\text{H}_2\text{SO}_4) = 3.5\text{ mol/L}$, $L/S = 10:1$, $T = 60\text{ }^\circ\text{C}$, $t = 60\text{ min}$); (c) Liquid-solid ratio ($C(\text{H}_2\text{SO}_4) = 3.5\text{ mol/L}$, $V(\text{H}_2\text{O}_2) = 0.8\%$ (v/v), $T = 60\text{ }^\circ\text{C}$, $t = 60\text{ min}$); (d) Leaching temperature ($C(\text{H}_2\text{SO}_4) = 3.5\text{ mol/L}$, $V(\text{H}_2\text{O}_2) = 0.8\%$ (v/v), $L/S = 10:1$, $t = 60\text{ min}$); (e) Leaching time ($C(\text{H}_2\text{SO}_4) = 3.5\text{ mol/L}$, $V(\text{H}_2\text{O}_2) = 0.8\%$ (v/v), $L/S = 10:1$, $T = 60\text{ }^\circ\text{C}$).

The concentration of sulfuric acid significantly influenced the leaching efficiencies of Li, Ni, Co, and Mn, as depicted in Figure 5a. As the concentration of sulfuric acid increased from 0.5 mol/L to 3.5 mol/L, the leaching efficiencies of these metals improved significantly, exceeding 94%. However, a further increase to 4.5 mol/L did not yield substantial changes in their leaching efficiencies.

Figure 5b demonstrates the effect of oxidant concentration on the leaching efficiencies of Li, Ni, Co, and Mn. With an increase in oxidant concentration from 0.2% (v/v) to 0.8% (v/v), the leaching efficiencies rose from 72%, 58%, 55%, and 68% to 94%, respectively. Increasing the oxidant concentration to 1.1% (v/v) resulted in only marginal improvements in these efficiencies. The Eh-pH diagram for the Li, Ni, Co, Mn- H_2O system (Figure 6) reveals that under acidic conditions ($\text{pH} < 4$), the metals can solubilize as ions within an oxidation potential range of -0.2 V to 1.2 V , emphasizing the critical role of the oxidant in enabling simultaneous leaching.

Additionally, enhancements in leaching efficiencies were observed with increases in the L/S ratio, temperature, and leaching time. Optimal conditions— L/S ratio of 10:1, temperature of $60\text{ }^\circ\text{C}$, and leaching time of 60 min—yielded leaching efficiencies of 96.58% for Li, 96.13% for Ni, 95.22% for Co, and 94.24% for Mn. Therefore, the best leaching parameters were determined as an H_2SO_4 concentration of 3.5 mol/L, an L/S ratio of 10:1, a leaching temperature of $60\text{ }^\circ\text{C}$, a leaching time of 60 min, and an H_2O_2 concentration of 0.8% (v/v).

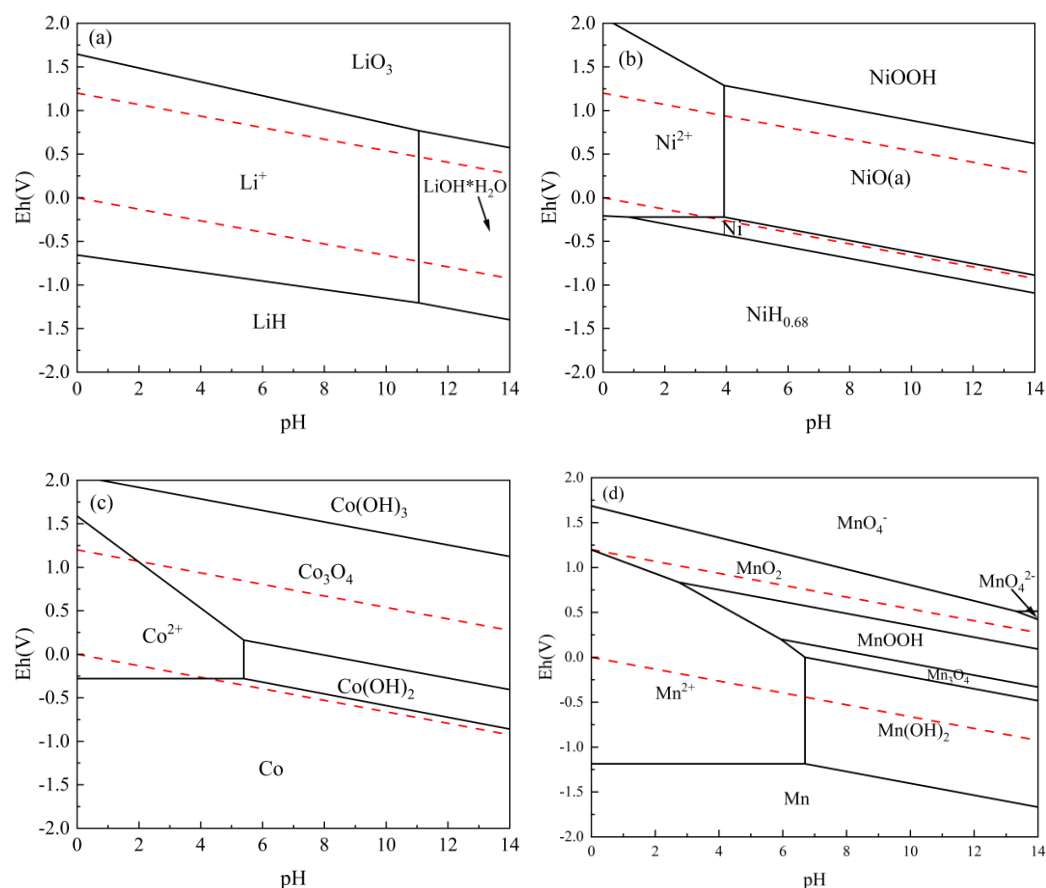


Figure 6. Eh–pH of each metal–H₂O system at 60 °C; (a) Li–H₂O; (b) Ni–H₂O; (c) Co–H₂O; (d) Mn–H₂O.

The XRD pattern shown in Figure 7 indicates that C was the primary phase identified in the leaching residue. The leaching solution (LA1) contained concentrations of Li, Ni, Co, and Mn at 2318, 6973, 2839, and 11,560 ppm, respectively (Table 2). The presence of impurity metals, such as Fe and Cu, leached at concentrations of 445 ppm and 537 ppm, added complexity to the subsequent separation process.

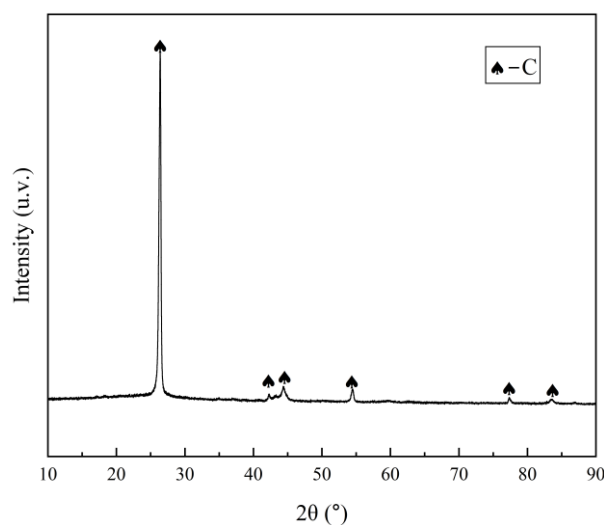


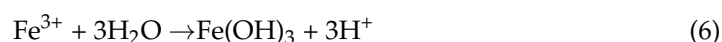
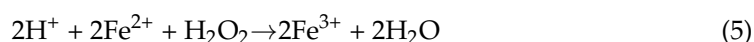
Figure 7. XRD pattern of leaching residue.

Table 2. Composition and concentration of each metal in the leach solution.

	Elemental Concentration (ppm)							V (mL)	pH
	Al	Fe	Cu	Li	Ni	Co	Mn		
LA1	522	445	537	2318	6973	2839	11,560	295	0.12
LA2	515	2403	43	2084	6213	2530	10,210	328	0.12
LA3	45	133	42	1754	5461	2302	10,100	364	3.50

(LA1: the leach solution; LA2: the solution of copper removal; LA3: the initial purification solution).

To address this, iron powder was added to the filtrate at 2 times the theoretical amount required to displace and remove copper. Following copper removal, 1% (*v/v*) hydrogen peroxide was added to the solution (LA2), and the pH was adjusted to 3.5 to precipitate iron (Equations (5) and (6)). This resulted in an initially purified solution (LA3) with concentrations of Cu and Al below 45 ppm and Fe at 133 ppm. Although the adsorption by generated Fe (OH)₃ and Al (OH)₃ [33] precipitates reduced the Li concentration to 1754 ppm, the low concentrations of Fe and Al limited this effect.



3.2. Selective Separation of Mn

Figure 8a illustrates the varied response of metal precipitation efficiencies to changes in pH. The precipitation efficiency of Mn remained stable across varying pH levels, while Co showed a more dynamic response; its efficiency initially increased, then decreased slightly, before increasing again. The efficiencies of Ni and Li loss exhibited minimal fluctuation, consistently remaining below 3% and 1%, respectively. Notably, at a pH of 2, Co's loss efficiency peaked at 18.36%, whereas Mn's precipitation efficiency was high at 98.47%, identifying pH 2 as the optimal condition for Mn precipitation.

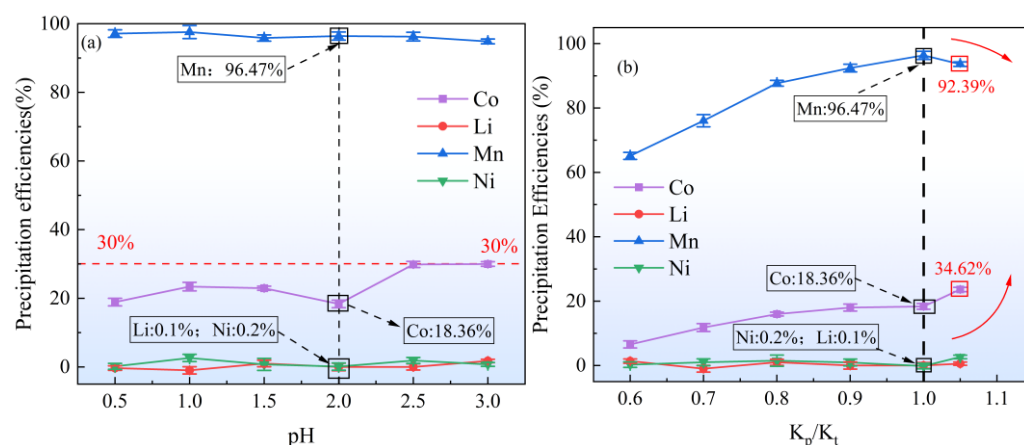


Figure 8. Effect of (a) pH on the precipitation efficiency of Mn ($T = 30\text{ }^{\circ}\text{C}$; $K_p/K_t = 1$; $t = 30\text{ min}$); (b) KMnO_4 dosage on the precipitation efficiency of Mn ($T = 30\text{ }^{\circ}\text{C}$; $\text{pH} = 2$; $t = 30\text{ min}$).

Figure 8b details how the KMnO_4 dosage ratio (actual amount (K_p)/theoretical amount (K_t), mol/mol) impacts Mn's precipitation efficiency. This efficiency plateaued as the ratio neared 0.9 and peaked at a 1:1 ratio, where Mn's precipitation efficiency was 98.47%. However, an increase in the ratio to 1.05 led to decreased efficiency, likely due to an over-addition of the reagent, resulting in a higher residual Mn concentration in the solution. Concurrently, the loss efficiencies of Li, Ni, and Co increased with the K_p/K_t ratio. At a

ratio of 1, Li and Ni exhibited loss efficiencies of 0.1% and 0.2%, respectively. The loss efficiency of Co varied significantly, ranging from 12.46% to 44.36%. Under these conditions, the Mn concentration in the solution was successfully reduced from 10,100 ppm to below 357 ppm (Table 3). The potential chemical reactions involved are outlined in Equation (7).

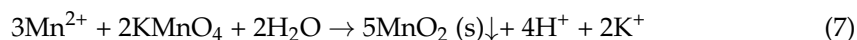


Table 3. Elemental Concentrations of Ni, Co, Mn, and Li in the leaching and filtrating solutions after precipitation.

	Elemental Concentration (ppm)				V (mL)	pH
	Li	Ni	Co	Mn		
LA3	1754	5461	2302	10,100	364	2.00
LA4	1752	5450	1879	357	370	2.50

(LA3: initial purification solution; LA4: filtered solution after Mn precipitation).

Eh–pH diagram of Mn–Co–H₂O at 30 °C is depicted in Figure 9, where the green region in the upper left corner represents the overlap of soluble Co (II) and Mn precipitation below the O₂ formation line (indicated by the upper dashed line). This narrow working range of Eh and pH values indicates the challenge in obtaining high-purity MnO₂ in the presence of Co²⁺, which is prone to oxidizing and forming Co₃O₄ precipitates, as demonstrated by Equation (8) and confirmed by experimental results.

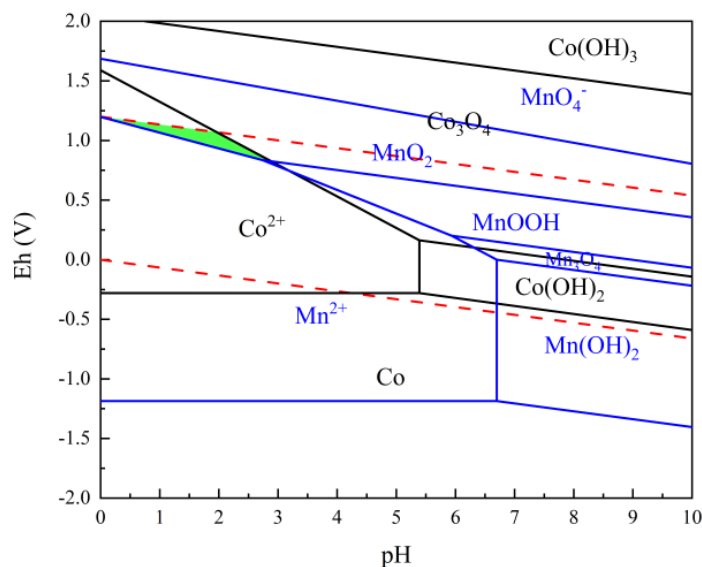


Figure 9. Eh–pH diagram of Mn–Co–H₂O at 30 °C.

In the experiments, the leaching solution was adjusted to a pH of 2 and then subjected to constant temperature stirring in a water bath, with the addition of solid potassium permanganate at a K_p/K_t ratio of 1:1. This addition produced a brown precipitate, which persisted until the reaction's completion. The solution was then filtered; the filter residue was dried for XRD analysis, and a quantitative sample of the filter residue was taken to determine the metal composition and content, as shown in Figure 10 and Table 4. The analysis of the filtrate's physical phase confirmed the presence of MnO₂ crystals, indicating the adequate precipitation of Mn²⁺ by potassium permanganate, thereby validating the experimental approach.

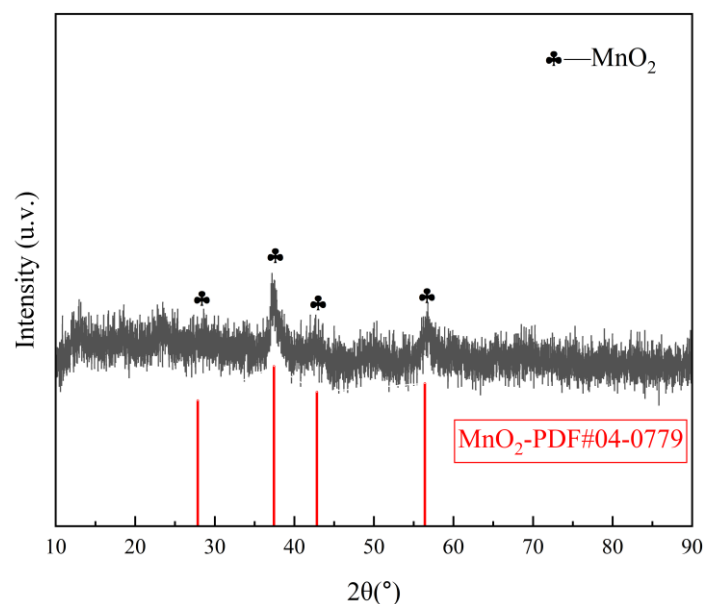
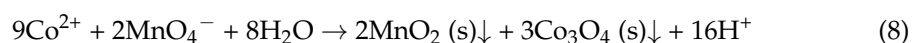


Figure 10. The XRD diffractogram pattern of filter sludge after precipitating Mn.

Table 4. Metal compositions of MnO₂ precipitation slag melt samples (wt %).

Element	Li	Ni	Co	Mn	Al	Fe	Cu
Content	0.01	0.59	2.51	54.53	0.00	1.14	0.28

However, the process also resulted in the co-precipitation of some Co²⁺. This finding aligns with the Eh-pH diagram, which predicts the formation of Co₃O₄. Despite this, due to the low concentration of Co₃O₄, it was not detected in the XRD analysis, indicating a minimal presence within the precipitate. Although cobalt accompanied the precipitation rate of 18.37% at a K_p/K_t of 1, it was significantly lower than the conventional neutralization and precipitation process, in which cobalt loss was greater than 40%, and the precipitation product had a Mn/Co mass ratio of 15.8:1, indicating that the MnO₂ precipitation is still highly selective for manganese.



3.3. Selective Recovery of Ni and Co

The post-precipitation filtration solution (LA4) contained high concentrations of Li, Ni, and Co. By adjusting the pH, these metals could be selectively extracted from the solution through stepwise extraction. The study explored the impact of different extractants on the extraction efficiencies of Li, Ni, and Co from acidic solutions, utilizing P204, P507, and Cyanex272. Within a pH range of 2.5 to 6.5, under extraction conditions of 30 °C and 20 min, the efficiencies of these processes were examined and are displayed in Figure 11a–c. These results indicated that P507 and Cyanex272 were more effective for Co extraction than P204. Notably, Co extraction with P507 led to a Li loss efficiency of about 25%, which was relatively constant across the pH range tested. Furthermore, the separation efficiency of Ni and Li using Cyanex272 was superior to that achieved with P507, suggesting its potential utility in segregating Co, Ni, and Li.

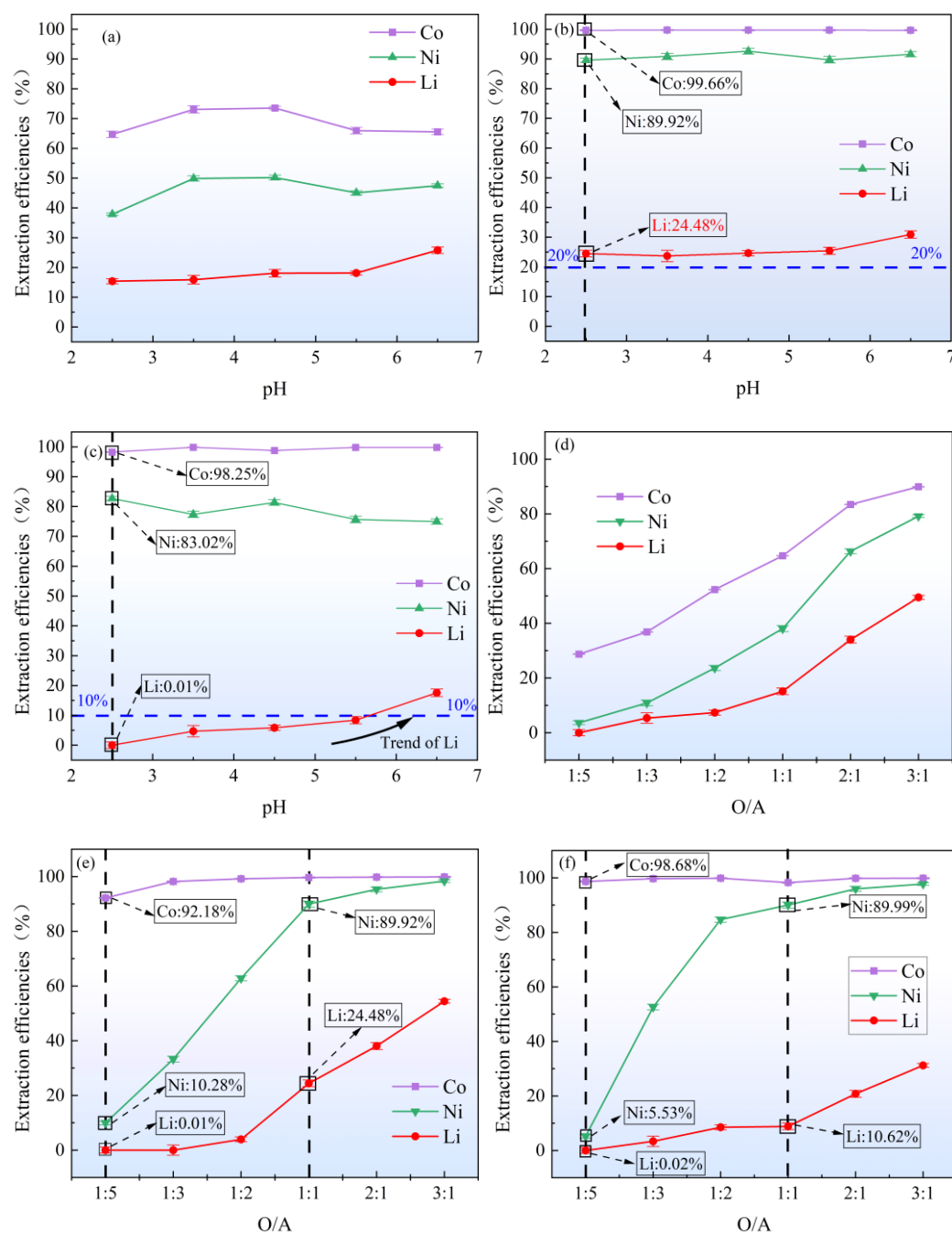


Figure 11. Metal extraction efficiencies as a function of pH for different extractants: (a) 20% P204 + 10% TBP + 70% sulfonated kerosene, 60% saponification efficiency; (b) 30% P507 + 70% sulfonated kerosene, 60% saponification efficiency; (c) 10% Cyanex272 + 10% TBP + 80% sulfonated kerosene, 50% saponification efficiency; Metal extraction efficiencies as a function of O/A ratio for different extractants: (d) 20% P204 + 10% TBP + 70% sulfonated kerosene, 60% saponification efficiency; (e) 30% P507 + 70% sulfonated kerosene, 60% saponification efficiency; (f) 10% Cyanex272 + 20% TBP + 80% sulfonated kerosene, 50% saponification efficiency. ($t = 20$ min, $T = 30$ °C).

Further analysis was conducted to evaluate the impact of varying the organic-to-aqueous (O/A) phase ratio from 1:5 to 3:1 on the extraction efficiencies of Li, Ni, and Co using these extractants, as shown in Figure 11d–f. This analysis revealed that pH was not a selective factor for Ni, Co, and Li extraction, and the selective extraction efficiency of Co by P507 and Cyanex272 was higher. However, as the O/A ratio increased, so did the extraction efficiencies of Ni and Li, which negatively affected the separation of Co from solutions containing Ni and Li.

The extraction effects of Cyanex272 on Co, Ni, and Li across various O/A ratios were distinct, leading to the selection of Cyanex272 as the preferred extractant for separating these metals. Under optimized conditions—a pH of 2.5, a saponification efficiency of 50%, an extraction temperature of 30 °C, an extraction time of 20 min, and an O/A ratio of 1:5, the extraction efficiency for Co reached 98.68%, while the loss efficiency for Ni was 5.53%, and Li was almost non-extractable. The concentrations of the metals in the aqueous phase before and after the extraction of Co and Ni are detailed in Table 5.

Table 5. Concentrations of metals in the aqueous phase before and after liquid extraction of Co and Ni after Mn precipitation, and in the aqueous phase of Li and Li stripping from Ni and Co residuals.

	Elemental Concentration (ppm)				pH
	Li	Ni	Co	Mn	
LA4	1752	5450	1879	357	2.5
LA5	1750	5149	25.2	46.7	2.5
LA6	1600	52.1	5.3	2.6	2.5

(LA4: the solution after precipitation of Mn; LA5: The remainder solution after extraction of Co; LA6: the solution after extraction of Co and Ni).

Following the successful extraction of Co using Cyanex272, the solution (LA5) was treated with a blend of extractants composed of 10% Cyanex272 + 10% TBP + and 80% sulfonated kerosene to separate and enrich Ni from Li. This step leveraged the superior separation efficiency of Cyanex272 at lower pH values compared to P204 and P507. Under conditions of 50% saponification efficiency, an extraction temperature of 30 °C, and an extraction duration of 20 min, the impact of varying the O/A phase ratio from 1:5 to 3:1 on the extraction efficiencies of Ni and Li was examined. The results are displayed in Figure 12.

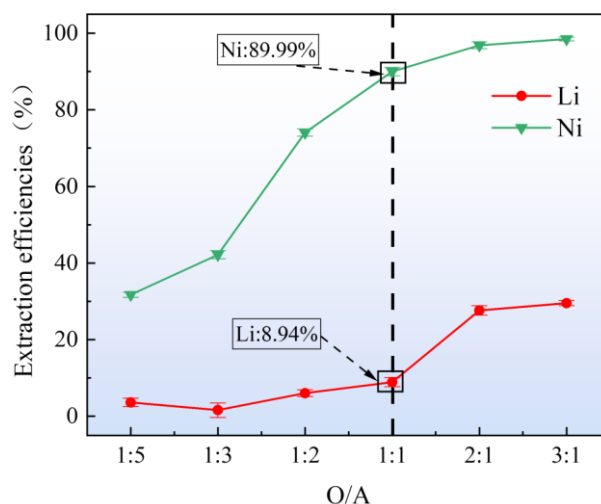
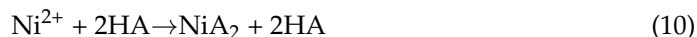


Figure 12. Ni extraction efficiency and Li loss efficiency of the solution extraction of Co at different O/A (saponification efficiency = 50%, T = 30 °C, t = 20 min).

As the O/A ratio increased, both Ni and Li extraction efficiencies also rose, with the growth in Ni extraction outpacing that of Li. This differential in extraction growth rates facilitates the effective separation of Ni from Li. Before reaching an O/A ratio of 1:1, the efficiency of Ni extraction consistently improved, while Li losses remained below 9%. However, beyond an O/A ratio of 1:1, the increase in Ni extraction efficiency began to plateau, and the loss efficiency of Li escalated to 27.72%.

These observations indicate that the optimal O/A ratio for achieving effective separation of Ni and Li is 1:1. The specific chemical reactions involved in this extraction process are represented by Equations (9) and (10), with HD denoting the extractant Cyanex272.



3.4. Li Enrichment and Recovery

After the extraction of Ni and Co, residual Li in the solution (LA6) necessitated a focused recovery effort due to its relatively low concentration of 1.6 g/L. HBL121 was chosen as the extractant for enriching Li. The extraction conditions were optimized to include a 30% HBL121 (v/v), an O/A of 1:1, an extraction temperature of 30 °C, and a duration of 10 min. The impact of pH on the Li extraction efficiency was thoroughly investigated, with results presented in Figure 13a. Notably, Li extraction efficiency remained extremely low, nearly zero, within the pH range of 10 to 12. However, Li extraction efficiency surged at a pH above 12, reaching over 95% at a pH of 13.5, which was determined to be the optimal pH for extraction.

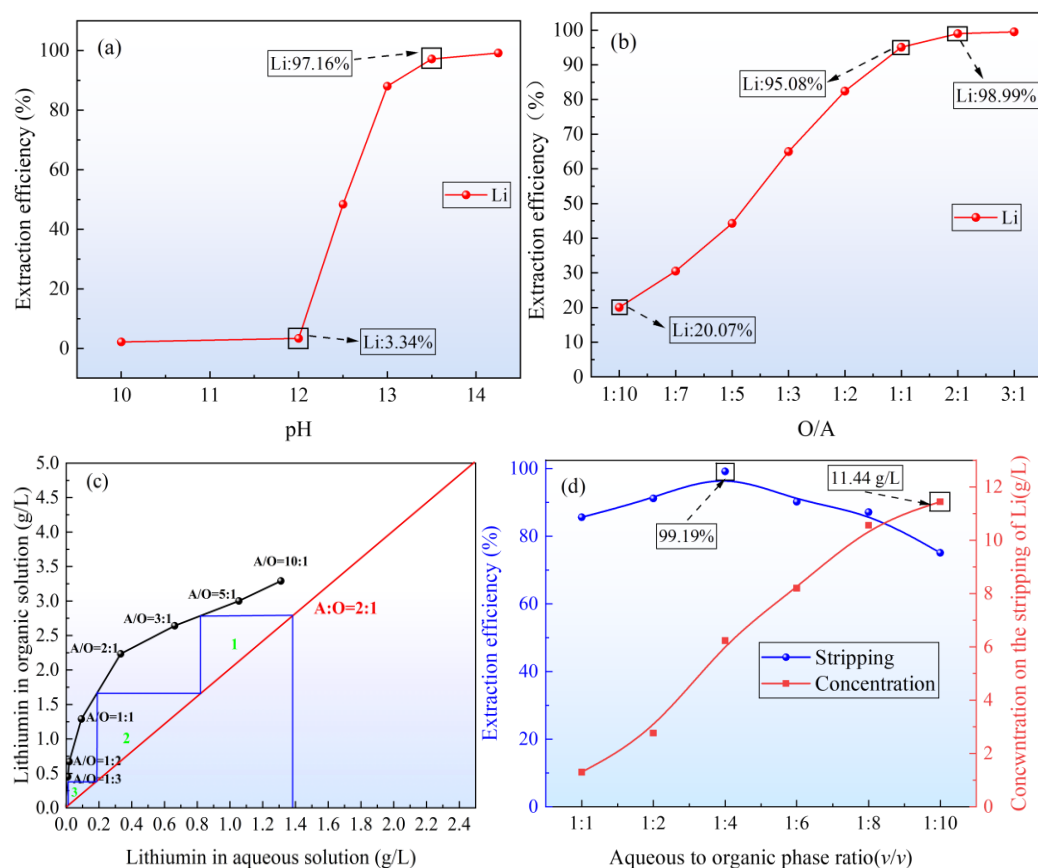


Figure 13. (a) Extraction efficiency of Li versus solution pH (O/A = 1:1, T = 30 °C, t = 10 min); (b) Extraction efficiency of Li versus O/A (T = 30 °C, t = 10 min); (c) McCabe–Thiele diagram for Li extraction with 30% (v/v) HBL121 in kerosene at 30 °C; (d) Stripping of Li from loaded organic phases versus compared to A/O (2 mol/L H₂SO₄, T = 30 °C, t = 10 min).

Further exploration of the influence of varying the O/A ratio on Li extraction showed significant findings, as illustrated in Figure 13b. As the O/A ratio increased from 1:10 to 1:1, Li extraction efficiency rose dramatically from 20.07% to 95.08%. Beyond this ratio, the increase in extraction efficiency plateaued, with minimal gains observed at a ratio of 3:1.

Given these findings, an O/A ratio of 1:1 was selected as optimal for the efficient stripping of the loaded organic phase, as higher ratios may complicate the process. The extraction isotherms under different conditions, depicted in Figure 13c, indicated that achieving a theoretical extraction efficiency of 99.5% for Li at 25 °C would require a three-stage countercurrent extraction process at an O/A ratio of 1:3.

A solution of 2 mol/L H₂SO₄ was employed to strip the loaded organic phase. Exploring different O/A ratios, from 1:1 to 1:10, showed that the Li extraction efficiency peaked at an O/A ratio of 1:1, as depicted in Figure 13d and summarized in Table 6. Remarkably, the concentration of Li in the enriched solution (LA8) reached 11.44 g/L at an O/A ratio of 1:10, demonstrating adequate Li enrichment and recovery.

Table 6. Concentration of metals in the aqueous phase before and after Li extraction and Li stripping.

	Elemental Concentration (ppm)				pH
	Li	Ni	Co	Mn	
LA6	1600	52.1	5.3	2.6	2.5
LA7	82.7	<1	<1	<1	13.5
LA8	11,443	<1	<1	<1	13.5

(LA6: the solution after extraction of Co and Ni; LA7: the solution after extraction of Li; LA8: the solution rich of Li).

The chemical reactions involved in this process are represented by Equations (11) and (12), where HD symbolizes the extractant HBL121.



Comparing the Fourier transform infrared spectra of the HBL121 extractant before and after lithium loading in Figure 14, the peaks at 1605 cm^{−1} and 1566 cm^{−1} are enhanced after loading, while the symmetric peaks at 700 and 770 cm^{−1} in the fingerprint region disappear, indicating that the C=N bond plays an important role in the extraction process. Simultaneously indicating that N–H is replaced to form a new complex N–Li, while other characteristic peaks show no significant changes.

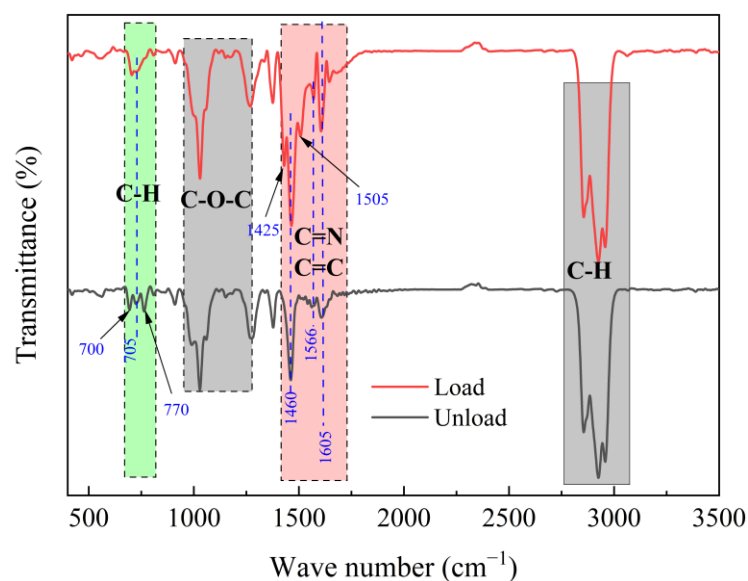


Figure 14. FTIR of HBL121 extractant load and unload lithium.

3.5. Flowsheet Development

Based on the research presented, a conceptual flowchart for separating Mn from spent high-Mn LIBs, alongside the concurrent recovery of Li, Ni, and Co, was developed, as depicted in Figure 15. Valuable metals, including Li, Ni, Co, and Mn, are initially extracted into a solution via H_2SO_4 and H_2O_2 leaching. Following this, Mn is selectively precipitated using KMnO_4 due to the high concentration of Mn (II) in the leachate. Subsequently, the remaining metals—Li, Ni, and Co—are sequentially separated from the solution after the Mn precipitation by adjusting the pH to appropriate levels and employing a specific extractant. This process is repeated to further enrich the extraction residue with Li. This methodology facilitates the effective separation and recovery of critical metals such as Li, Ni, Co, and Mn from spent high-Mn LIBs.

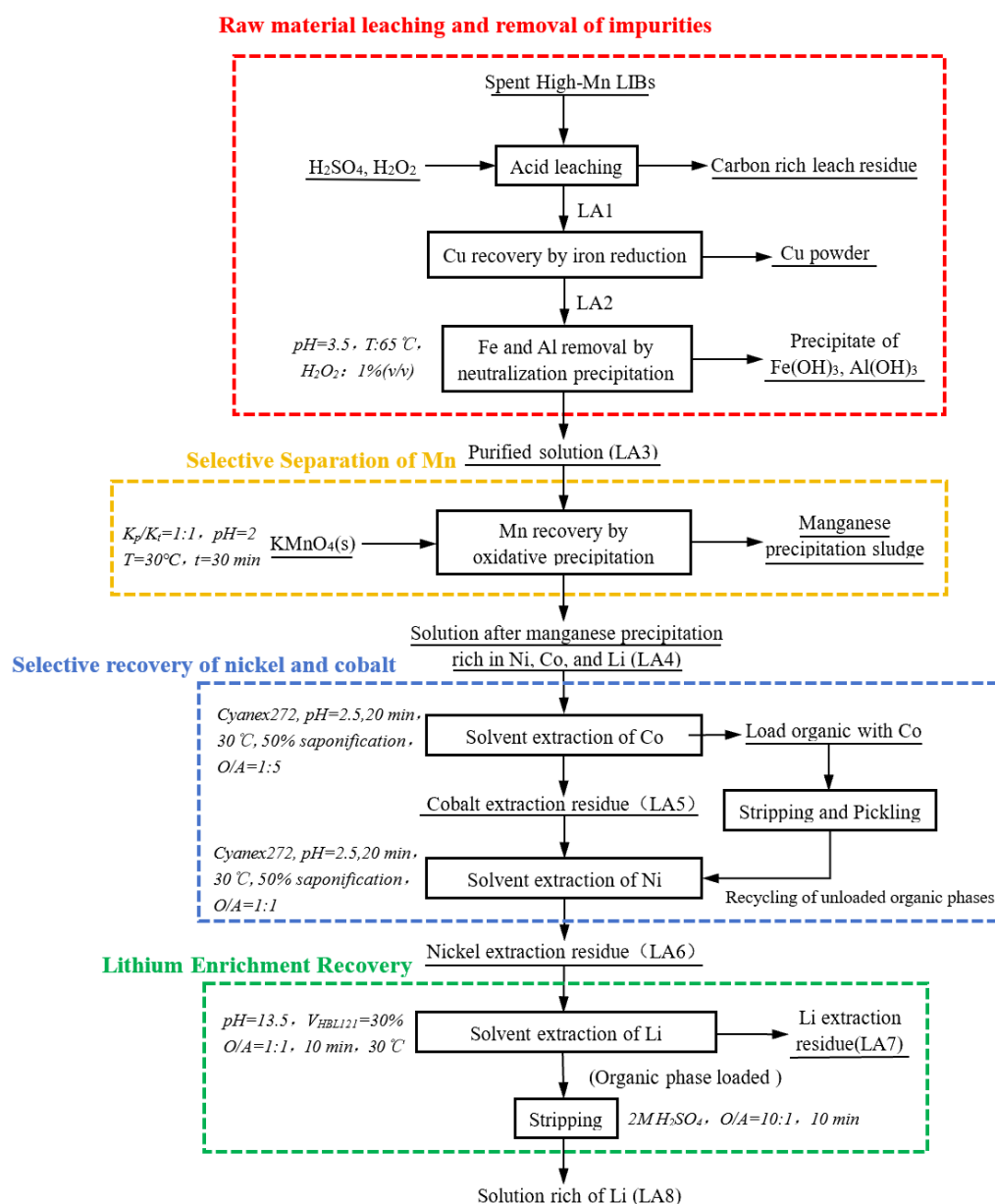


Figure 15. Proposed flow sheet for separation and recovery of Ni, Co, Mn, and Li from spent high-Mn lithium-ion batteries.

4. Conclusions

A process for systematically recovering valuable metals from spent LIBs has been proposed, achieving selective separation of Ni, Co, and Mn. Priority Mn precipitation can

separate large amounts of Mn at once, with high efficiency, a shortened process, and simple operation. Moreover, Li enrichment can be achieved without the need for evaporation crystallization. The process primarily includes Mn oxide precipitation separation, Ni and Co cascade separation, and Li short-process enrichment. The technology presents significant technical and economic advantages over conventional recycling routes by minimizing lithium loss and streamlining Mn separation. Key process achievements include:

- (1) The leaching of valuable metals was achieved by using H_2SO_4 and H_2O_2 , and leaching efficiencies of Li, Ni, Co, and Mn were reached 96.58%, 96.13%, 95.22%, and 94.24%, respectively, under optimal conditions which were $C(\text{H}_2\text{SO}_4)$ of 3.5 mol/L, $V(\text{H}_2\text{O}_2)$ of 0.8% (v/v), L/S of 10:1, temperature of 60 °C, and time of 60 min.
- (2) Directional precipitation of Mn can be realized by using KMnO_4 , and precipitation efficiency of Mn as MnO_2 via redox control was achieved 98.47% at a pH of 2 and with the K_p/K_t ratio of 1:1.
- (3) Stepwise separation of Ni and Co can be realized by using the extractant Cyanex272, as well as Ni and Co were extracted 98.68% and 89.99% at a pH of 2.5 and with an O/A of 1:5 (the extraction O/A of Ni was 1:1).
- (4) Selective separation of Li was achieved by using the extractant HBL121, and over 95.00% of Li can be extracted at pH 13.5 with an O/A ratio of 1:1. The Li concentration was enriched from 1.60 g/L to 11.44 g/L.

The combined high recovery rates, operational simplicity, and minimal reliance on costly inputs underscore the process's substantial potential for cost-effective industrial upscaling and sustainable resource circularity.

Author Contributions: Conceptualization, F.L., C.L. and J.Z.; data curation, J.Z.; formal analysis, J.Z.; funding acquisition, F.L. and C.L.; investigation, J.Z.; methodology, F.L. and J.Z.; software, F.L. and C.L.; resources, F.L. and C.L.; validation, J.Z., F.C., T.Z., H.W. and Y.G.; visualization, J.Z.; writing—original draft preparation, J.Z.; writing—review and editing, F.L. and C.L.; supervision, F.L., C.L., F.C., T.Z., H.W. and Y.G.; project administration, F.L. and C.L.; All authors have read and agreed to the published version of the manuscript.

Funding: This paper has been financially supported by Jiangxi Ganpo Talent Plan Innovative High end Talent Project (gpyc20240066), the Natural Science Foundation for Distinguished Young Scholars of Jiangxi Province (No. 20232ACB214006), Training Plan for Academic and Technical Leaders of Major Disciplines in Jiangxi Province (20225BCJ23009), Major Science and Technology Research Projects in Yichun City (2023ZDKJGG01), Unveiling and commanding project in Jiangxi Province (20213AAE02010), Postdoctoral Innovative Talent Support Program of Shandong Province and Program of Qingjiang Excellent Young Talents, Jiangxi University of Science and Technology (No. JXUSTQJYX2019006), Jiangxi Postdoctoral Science Foundation (No. 2019 KY07), and Jiangxi Provincial Key Laboratory of High-Performance Steel and Iron Alloy Materials (No. 2024SSY05041).

Data Availability Statement: The original contributions presented in the study are included in the article; further inquiries can be directed to the corresponding authors.

Conflicts of Interest: The authors declare no conflicts of interest. The authors declare that they have no known competing financial interests or personal relationships that could have appeared to influence the work reported in this paper.

References

1. Gu, K.; Gu, X.; Wang, Y.; Qin, W.; Han, J. A green strategy for recycling cathode materials from spent lithium-ion batteries using glutathione. *Green Chem.* **2023**, *25*, 4362–4374. [\[CrossRef\]](#)
2. Palacín, M.R.; de Guibert, A. Why do batteries fail? *Science* **2016**, *351*, 1253292. [\[CrossRef\]](#)
3. Zhang, Y.; Ning, P.; Yang, X.; Dong, P.; Lin, Y.; Meng, Q. New progress in research on recycling technology of waste ternary lithium-ion batteries. *Chem. Ind. Eng. Prog.* **2020**, *39*, 2828–2840. [\[CrossRef\]](#)

4. Yang, K.; Xiong, Z.Y.; Liu, Z.L.; Xu, Z.F.; Wang, R.X.; Nie, H.P. Study on the recovery of Li by reduction roasting of used ternary lithium-ion battery cathode. *J. Cent. South Univ. (Sci. Technol.)* **2020**, *51*, 3367–3378. [\[CrossRef\]](#)
5. Hu, G.C.; Hu, N.H.; Wu, J.J.; Ma, W.H. Research progress in recovery of valuable metals in cathode materials for lithium-ion batteries. *Chin. J. Nonferrous Met.* **2021**, *31*, 3320–3343. [\[CrossRef\]](#)
6. Natarajan, S.; Aravindan, V. Burgeoning Prospects of Spent Lithium-Ion Batteries in Multifarious Applications. *Adv. Energy Mater.* **2018**, *8*, 1802303. [\[CrossRef\]](#)
7. Zhong, X.H.; Chen, L.L.; Han, J.W.; Liu, W.; Jiao, F.; Qin, W.Q. Overview of present situation and technologies for the recovery of spent lithium-ion batteries. *Chin. J. Eng.* **2021**, *473*, 161–169. [\[CrossRef\]](#)
8. Wang, C.; Liu, W.; Yang, C.; Ling, H. Extraction of Valuable Metals from Spent Li-Ion Batteries Combining Reduction Smelting and Chlorination. *Metals* **2025**, *15*, 732. [\[CrossRef\]](#)
9. Batkal, A.; Kamunur, K.; Mussapyrova, L.; Milikhhat, B.; Nadirov, R. Optimized Ammonia Leaching and Energy-Efficient Stripping for Lithium and Cobalt Recovery from Spent LiCoO₂ Cathodes. *Metals* **2025**, *15*, 690. [\[CrossRef\]](#)
10. Wang, D.B.; Liang, J.L.; Deng, X.C. Research status of extraction and recovery of lithium resources and preparation process of lithium. *Inorg. Chem. Ind.* **2020**, *52*, 8–12. [\[CrossRef\]](#)
11. Wang, Y.B.; Guo, Y.W.; Sun, C.; Ruan, J.L.; Zhang, J.Q. Discussion on environmental risk analysis and management counter measures of waste power batteries recovery in China. *J. Environ. Eng. Technol.* **2019**, *9*, 207–212. [\[CrossRef\]](#)
12. Chen, L. Research on Resourceful Recycling of Nonferrous Metals in Waste Lithium-Ion Batteries. Master's Thesis, Central South University, Changsha, China, 2011. Available online: <https://d.wanfangdata.com.cn/thesis/Y1916201> (accessed on 16 March 2012).
13. Wang, Z.Y.; Wang, B.X.; Yuan, W.L.; Yu, X.; Zhao, Y.; Song, Y.H.; Ma, H.Z. Experimental study on the recovery of nickel-cobalt-manganese from waste lithium-ion batteries. *Hydrometall. China* **2022**, *41*, 427–432. [\[CrossRef\]](#)
14. Xu, Z.H.; Liu, Z.D.; Wang, S.B.; Lu, Z.G.; Zhang, Z.T.; Wang, H.; Jiang, F. Review on hydrometallurgical recovery of valuable metals from spent lithium-ion batteries. *J. China Univ. Min. Technol.* **2022**, *51*, 454–465. [\[CrossRef\]](#)
15. Xuebin, P. Research on New Process of Wet Recovery of Valuable Metals from Waste Nickel-Cobalt-Manganese Ternary Lithium Battery Cathode Materials. Ph.D. Thesis, Kunming University of Science and Technology, Kunming, China, 2023.
16. Gu, K.Q.; Tan, W.Q.; Han, J.W. Reduction leaching of valuable metals from spent cathode materials of lithium batteries using orange peel. *Chin. J. Nonferrous Met.* **2024**, *34*, 561–572. [\[CrossRef\]](#)
17. Dai, M.; Zhang, Y.; Zhang, K.; Zhao, Y.B. Recovery of Cobalt, Nickel and Lithium From Spent Lithium Ion Battery Cathode Material by Solvent Extraction--Precipitation. *Hydrometall. China* **2019**, *38*, 276–282. [\[CrossRef\]](#)
18. Li, C.; Dai, G.; Liu, R.; Wang, C.; Wang, S.; Ju, Y.; Jiang, H.; Jiao, S.; Duan, C. Study on Separation and Recovery of Nickel Cobalt Manganese Lithium from Waste Ternary Lithium Ion Batteries. *Sep. Purif. Technol.* **2023**, *306*, 122559. [\[CrossRef\]](#)
19. Zhang, T.; Liu, F.; Chen, H.; Chen, Z.; Liao, C.; Chen, F.; Guo, Y. Cleaner Process for the Selective Extraction of Lithium from Spent Aluminum Electrolyte Slag. *ACS Sustain. Chem. Eng.* **2024**, *12*, 11797–11808. [\[CrossRef\]](#)
20. Jiang, L.; Zhan, L.; Zhang, Q.Z. Separation and recovery of lithium Co Ni manganese from acidic leachate of cathode active materials of used ternary batteries. *Chin. J. Nonferrous Met.* **2020**, *30*, 2684–2694. [\[CrossRef\]](#)
21. Zhong, X.H.; Jiao, F.; Liu, T.; Tan, W.Q. Overview of recovery technology for spent Li-ion battery. *Battery Bimon.* **2018**, *48*, 63–67. [\[CrossRef\]](#)
22. Tang, C.; Shan, W.; Zheng, Y.; Zhang, L.; Liu, Y.; Liao, B.; Chen, H.; Hou, X. Recovery of Li/Co from spent lithium-ion battery through iron-air batteries. *Chem. Eng. J.* **2024**, *502*, 157578. [\[CrossRef\]](#)
23. Dong, B.; Tian, Q.H.; Xu, Z.P.; Li, D.; Wang, Q.A.; Guo, X.Y. Progress of research on clean extraction of Ni Co lithium resources for new energy strategic metals. *Mater. Rep.* **2023**, *37*, 127–141. [\[CrossRef\]](#)
24. Yang, C.; Zhang, Q.; Li, L.J.; Shen, Z.H. Study on the Separation of Manganese from a Low-grade Manganese Carbonate Ore in Guizhou. *Nonferrous Met.* **2020**, *3*, 58–66. [\[CrossRef\]](#)
25. Xu, Z.G.; Ji, S.J.; Wang, Z.H.; Qian, Z.D.; Wang, F.; Zhou, T. Research status of nickel-cobalt extraction and separation technology in solution. *Hydrometall. China* **2018**, *37*, 342–348. [\[CrossRef\]](#)
26. Guo, Y.; Liu, F.; Chen, F.; Chen, Z.; Zeng, H.; Zhang, T.; Shen, C. Recycling of Valuable Metals from the Priority Lithium Extraction Residue Obtained through Hydrogen Reduction of Spent Lithium Batteries. *Batteries* **2024**, *10*, 28. [\[CrossRef\]](#)
27. Wang, L.; Jiao, X.; Bian, H.; Ma, J.; Zhang, Z. Selective lithium recycling and regeneration from spent lithium-ion batteries via a sulfur roasting method. *Sep. Purif. Technol.* **2025**, *360*, 131236. [\[CrossRef\]](#)
28. Lei, S.; Ding, H.; Yuan, S.; Wen, G.; Han, C.; Dong, Z.; Wang, W. Prioritized recovery of lithium from spent lithium-ion batteries by synergistic roasting with Na₂SO₄: Precise regulation. *Sep. Purif. Technol.* **2025**, *360*, 131128. [\[CrossRef\]](#)
29. Kang, X.; Zhang, X.; Liu, S.; Shi, Y.; Wu, Y.; Li, J.; Zhang, H.; Xie, Y.; Qi, T. Selective recovery of lithium from used lithium-ion batteries spent via grain boundary reconstruction reaction. *Sep. Purif. Technol.* **2025**, *356*, 129726. [\[CrossRef\]](#)
30. Peng, Z.; Zhu, Z.; Li, J.; Lu, Q.; Wang, M. High selectivity and High-efficiency extraction lithium from spent lithium-ion batteries by solvothermal method with ammonium chloride. *Sep. Purif. Technol.* **2025**, *360*, 131298. [\[CrossRef\]](#)

31. Shi, H.; Zhang, J.; Ou, L. A comprehensive review on the separation and purification of valuable metals from the leachate of spent lithium-ion batteries. *Sep. Purif. Technol.* **2025**, *360*, 130847. [[CrossRef](#)]
32. Shuai, J.; Liu, W.; Rohani, S.; Wang, Z.; He, M.; Ding, C.; Lv, X. Efficient extraction and separation of valuable elements from spent lithium-ion batteries by leaching and solvent extraction: A review. *Chem. Eng. J.* **2025**, *503*, 158114. [[CrossRef](#)]
33. Zou, Y.; Chernyaev, A.; Seisko, S.; Sainio, J.; Lundström, M. Removal of iron and aluminum from hydrometallurgical NMC-LFP recycling process through precipitation. *Miner. Eng.* **2024**, *218*, 109037. [[CrossRef](#)]

Disclaimer/Publisher's Note: The statements, opinions and data contained in all publications are solely those of the individual author(s) and contributor(s) and not of MDPI and/or the editor(s). MDPI and/or the editor(s) disclaim responsibility for any injury to people or property resulting from any ideas, methods, instructions or products referred to in the content.